Clustering of T Cell Ligands on Artificial APC Membranes Influences T Cell Activation and Protein Kinase C θ Translocation to the T Cell Plasma Membrane[1]

Francesca Giannoni,[2*†] Joellen Barnett,[2*] Kun Bi,[†] Rodrigo Samodal,[*] Paola Lanza,[§] Patrizia Marchese,[‡] Rosario Billetta,[§] Randi Vita,[§] Mark R. Klein,[*¶] Berent Prakken,[*¶] William W. Kwok,[‖] Eli Sercarz,[#] Amnon Altman,[†] and Salvatore Albani[3*§]

T cell activation is associated with active clustering of relevant molecules in membrane microdomains defined as the supramolecular activation cluster. The contact area between these regions on the surface of T cells and APC is defined as the immunological synapse. It has been recently shown that preclustering of MHC-peptide complexes in membrane microdomains on the APC surface affects the efficiency of immune synapse formation and the related T cell activation. Disruption of such clusters may reduce the efficiency of stimulation. We describe here an entirely artificial system for Ag-specific, ex vivo stimulation of human polyclonal T cells (artificial APC (aAPC)). aAPC are based on artificial membrane bilayers containing discrete membrane microdomains encompassing T cell ligands (i.e., appropriate MHC-peptide complexes in association with costimulatory molecules). We show here that preclustering of T cell ligands triggered a degree of T cell activation significantly higher than the one achieved when we used either soluble tetramers or aAPC in which MHC-peptide complexes were uniformly distributed within artificial bilayer membranes. This increased efficiency in stimulation was mirrored by increased translocation from the cytoplasm to the membrane of protein kinase θ, a T cell signaling molecule that colocalizes with the TCR within the supramolecular activation cluster, thus indicating efficient engagement of T cell activation pathways. Engineered aAPC may have immediate application for basic and clinical immunology studies pertaining to modulation of T cells ex vivo. *The Journal of Immunology,* **2005, 174: 3204–3211.**

T cell activation requires direct contact between the TCR and the MHC-peptide complex on the surface of APC. TCR engagement induces active recruitment and clustering of relevant membrane receptors. This results in the formation of the supramolecular activation cluster (SMAC)[4] (1–5) within the T cell membrane. These events lead to the formation of the immunological synapse (IS) (6), a highly specialized area at the site of T cell-APC contact. Formation of the IS is important to mediate TCR signal transduction and achieve full T cell activation (7–11). Formation of the SMAC on the T cell membrane is induced in T cell hybridoma or naive transgenic T cells by employing a system of planar lipid bilayers in which MHC-peptide complexes and adhesion molecules are uniformly distributed. SMAC formation was found to correlate with cellular activation (12). Accumulation of MHC-peptide complexes at the APC-T cell interface was assumed to occur passively upon the interaction with the TCR. T cell activation was achieved when the average distance between MHC-peptide complexes was 20 nm or less (13) or when the density of MHC-peptide complexes was at least 60 molecules/μm^2 (5). One hundred to 200 MHC-peptide complexes per APC were the minimum number of complexes required to stimulate IL-2 production by T cells (14). Recently, ex vivo activation and expansion of CD8 T cells was also achieved by using beads coated with anti-CD3 Ab or HLA-peptide complexes (15).

Previously, we described artificial APC (aAPC) in which MHC-peptide complexes were randomly distributed within the aAPC membrane (16, 17). These aAPC were prepared by inserting affinity-purified MHC molecules containing their transmembrane domain in highly fluid lipid bilayers. Such aAPC were very efficient in identifying class II-restricted Ag-specific T cells but their capacity to effectively stimulate T cells was limited to some high-affinity T cell hybridomas which do not require costimulation. As also suggested by elegant work from others (18), using similar technology, suboptimal stimulatory capacity was presumably due to the combination of several factors, including inappropriate orientation of MHC molecules, lack of organization, and insufficient local concentration of T cell ligands in the area of contact between the aAPC and T cell. Taken together, these data show that the efficiency of these artificial systems in inducing T cell activation may be influenced by the relative density of MHC-peptide complexes available at the point of interaction.

*Departments of Medicine and Pediatrics, University of California, San Diego, CA 92093 and IACOPO Institute for Translational Medicine, San Diego/Utrecht; †La Jolla Institute for Allergy and Immunology, San Diego, CA 92121; ‡Department of Molecular and Experimental Medicine, The Scripps Research Institute, La Jolla, CA 92121; §Androclus Therapeutics, Milan, Italy; ¶Department of Pediatric Immunology, Wilhelmina Children's Hospital, University of Utrecht, University Medical Center Utrecht, Utrecht, The Netherlands; ‖Benaroya Research Institute, Virginia Mason, Seattle, WA 98101; and #Torrey Pines Institute for Molecular Studies, San Diego, CA 92121

Received for publication October 30, 2004. Accepted for publication December 21, 2004.

The costs of publication of this article were defrayed in part by the payment of page charges. This article must therefore be hereby marked *advertisement* in accordance with 18 U.S.C. Section 1734 solely to indicate this fact.

[1] This study was supported in part by National Institutes of Health Grants 5P50 AR44850-04, N01-AR-9-2241, 2R01 AI41721-05, and 1R01AR48084-01 and by a donation from Associazione Italiana Contro l'Artrite (Milan, Italy).

[2] F.G. and J.B. contributed equally to this work.

[3] Address correspondence and reprint requests to Dr. Salvatore Albani, Department of Pediatrics, University of California, 9500 Gilman Drive, San Diego, CA 92093-0663. E-mail address: salbani@ucsd.edu

[4] Abbreviations used in this paper: SMAC, supramolecular activation cluster; IS, immunological synapse; aAPC, artificial APC; CTB, cholera toxin B; NA, neutravidin; PKC, protein kinase C; HA, hemagglutinin; MD, microdomain; MDaAPC, aAPC cells with ligands organized into membrane MD; RT, room temperature.

Copyright © 2005 by The American Association of Immunologists, Inc.

0022-1767/05/$02.00

The concept that high relative density of T cell ligands may affect optimal stimulation was further corroborated by findings suggesting that MHC-peptide complexes are clustered on the surface of APC even in the absence of T cells (19–23). Disruption of these discrete microdomains (MDs) reduced the efficiency of natural APC in inducing T cell activation (19). This seems to be particularly true when polyclonal, lower affinity T cells are used.

We compared here two systems of aAPC, one in which MHC-peptide complexes were uniformly distributed on the aAPC surface and another in which MHC-peptide complexes were clustered in MDs on the aAPC surface and designated here as MDaAPC. The two types of aAPC were tested for their capability to induce ex vivo activation of human polyclonal Ag-specific $CD4^+$ T cells. The efficiency of activation by the two types of aAPC was compared with stimulation assays using natural APC or tetramers. We also explored whether migration of protein kinase C θ (PKCθ) to the SMAC could be induced by MDaAPC, thus indicating engagement of physiological pathways of T cell activation.

Altogether, our study in two completely artificial systems underscores the advantages of mimicking the naturally patchy distribution of T cell ligands on APC membranes to efficiently manipulate T cells. This technology provides a viable tool for the modulation and expansion ex vivo of Ag-specific T cells which are difficult to expand or may be scarcely represented. There are immediate implications for this approach for basic research as well as for clinical applications, such as cell therapy of immunodeficiencies and cancer.

Materials and Methods

Preparation of liposomes

Micelles were prepared from phosphatidylcholine (Sigma-Aldrich) and cholesterol (Sigma-Aldrich) in a molar ratio of 7:2, respectively. Lipids, dissolved in chloroform were dried under nitrogen and resuspended at 10 mg/ml in 140 mM NaCl and 10 mM Tris-HCl containing 0.5% sodium deoxycholate (Sigma-Aldrich) at pH 8.0. Monosialoganglioside GM1 (Sigma-Aldrich) was added at a final concentration of 0.28 or 0.55 mM. Before use, samples were sonicated and dialyzed against PBS for 48 h at 4°C.

Assembly of MDaAPC

MDaAPC were assembled by combining biotinylated Abs and MHC-peptide complexes with biotinylated cholera toxin B (CTB; Sigma-Aldrich) in a 3:1 molar ratio. Neutravidin (NA; Pierce) was added at a ratio of 1 mol of NA per 4 biotinylated moiety. After 15 min of incubation at room temperature (RT), the liposomes were added. This structure ensures proper orientation of T cell ligands. The number of GM1 sites available for binding by CTB subunits was determined by FACS. These corresponded closely to the calculated available sites based on the synthesis of the GM1-liposome. Several experiments were performed by sequentially adding the MD components to the liposomes and measuring binding by FACS. The GM1-containing liposomes bound either FITC-conjugated CTB or biotinylated CTB, visualized by streptavidin-CyChrome (BD Pharmingen). This binding could be blocked by preincubation with nonfluorescent avidin block (data not shown). To establish the optimal ratio between GM1 and TCR ligands in the MDs, a titration curve with different concentrations of anti-CD3 Ab or MHC/peptide was made. By using different CTB:GM1 molar ratios in a range from 1:0.1 to 1:100, the highest rate of binding was achieved with a molar ratio of 1:50 CTB:GM1. DRB1*0701 molecules were purified from a homozygous HLA-DRB1*0701 human B cell line by affinity chromatography (AminoLink-Pierce coupled with LB3.1 Ab from HB298 ATCC) as previously described (16). Affinity-purified DRB1*0701 molecules were biotinylated at the C terminus (EZLink Biotin-LC-PEO-Amine; Pierce); efficiency of biotinylation was measured spectrophotometrically using HABA avidin reagent (Sigma-Aldrich). The recombinant biotinylated HLADRB1*1101 molecule was purified from transfected S2 cells (24, 25). Binding of hemagglutinin (HA) 307–319 peptide to affinity-purified DRB1*0701 was performed for 72 h at RT; MHC-peptide binding parameters were previously optimized (16). Binding of $HA_{307–319}$ peptide with recombinant HLA-DRB1*1101 molecules was performed according to Kwok's protocol (24). Efficiency of binding between T cells and aAPC was measured by FACS as the percentage of the total $CD4^+$ T cells bound to the aAPC. This was visualized by labeling the aAPC with FITC-conjugated CTB before incubation with PBMC.

Evaluation of aAPC size by FACS

The average size of the liposomes was evaluated by comparison with yellow-green fluorescent beads of known size with diameters ranging between 0.1 and 1.0 μm (Fluoresbrite Micro particles; Polysciences). Liposomes particles were incubated with biotinylated CTB, which binds the GM1 moieties, washed, and then labeled with CyChrome-conjugated streptavidin. Liposomes were washed by centrifugation at 13,000 $\times$ *g* for 10 min at RT. Samples were prepared by mixing a known volume of the CyChrome-labeled liposomes with a known number of the Fluoresbrite Micro beads of different sizes (0.5, 0.75, and 1.0 nm in diameter). The samples were then acquired by FACS with the beads visualized in the FL1 channel and the streptavidin-CyChrome-labeled liposomes in the FL3 channel. The samples were counted for exactly 20 s and the liposome:bead ratio was calculated. Using this ratio, it was possible to obtain the number of liposome particles in 1 ml of the original sample by using the formula provided by the kit: number of particles per milliliter = $6W \times 1012/rxpxf3$, where W = grams of polymer, r = density of polymer in grams per milliliter, p = 3.1417, and f = diameters in micrometers of latex micro particles.

Preparation of tetramers

MHC-peptide tetramers were assembled using recombinant biotinylated HLA-DRB1*1101 molecules or affinity-purified biotinylated DRB1*0701 molecules, complexed with $HA_{307–319}$ peptide. Tetramers were formed by cross-linking of biotinylated DRB1*0701/$HA_{307–319}$ or biotinylated HLA-DRB1*1101-$HA_{307–319}$ complexes with NA and incubating for 2 h at RT (Pierce). The NA-MHC/peptide complex molar ration was 1:8, to ensure the occupancy of the four biotin binding sites of NA (24, 25).

Ex vivo stimulation of $CD4^+$ T cells

$CD4^+$ T cells were sorted from total PBMC using influenza-immunized donors with a FACSVantage cytometer (BD Biosciences). For each sample, 2.5 $\times$ 10^5 $CD4^+$ T cells were incubated for 60 h in RPMI 1640 containing 10% human Ab serum at 37°C in different stimulating conditions. For polyclonal T cell stimulation, cells were added to aAPCs carrying 45 pmol of anti-CD3 Ab alone or in combination with 45 pmol of anti-CD28 Ab on raft; aAPC with the same picomoles of anti-CD28 Ab or anti-CD19 Ab, loaded on rafts, were used as controls. $CD4^+$ T cells were also incubated in the presence of anti-CD3-coated beads (anti-CD3 MicroBeads MACS; Miltenyi Biotec) plus soluble purified anti-CD28 Ab (2 μg/ml; BD Pharmingen) or in 96-well plates coated with anti-CD3 plus soluble anti-CD28. The amounts of beads and Abs for the controls were calculated to stimulate the cells with the same picomoles of anti-CD3 and anti-CD28 Abs loaded on the aAPC (45 pmol for 2.5 $\times$ 10^5 cells).

For Ag-specific T cell stimulation, 2.5 $\times$ 10^5 sorted $CD4^+$ T cells were incubated for 60 h with aAPC carrying 125 pmol of biotin-DRB1*0701/or biotin-HLA-DRB1*1101/$HA_{307–319}$ complexes on MD alone or in combination with 75 pmol of anti-CD28 Ab at 37°C. As controls, aAPC with the same number of moles of anti-CD28 Ab or anti-CD19 Ab, loaded on rafts, were used. Stimulation was also induced by incubating $CD4^+$ T cells with aAPC containing MHC-peptide complexes randomly distributed in the membrane. In this case, 125 pmol of the same MHC-peptide complexes without biotinylation were directly inserted and uniformly distributed on the aAPC surface (16).

For stimulation with tetramers, after cross-linking of the biotinylated MHC/peptide with NA, the tetramer solution was directly added to 2.5 $\times$ 10^5 sorted $CD4^+$ T cells and incubated for 60 h at 37°C.

After stimulation, cells were stained with PE-conjugated anti-CD69 mAb (BD Pharmingen) or permeabilized, fixed, and stained with PE-conjugated anti-IL-2 mAb (BD Pharmingen). Analysis was performed with CellQuest software (BD Biosciences).

Ex vivo stimulation of human $HA_{307–319}$-specific human T cell line by MDaAPC or natural APC

The immortalized human T lymphoid cell line CH7C17 was cultured for 10 days in a selection medium. The Vβ3 TCR of the CH7C17 cell line was stained every 3 days with mouse anti-human TCR Vβ3 FITC (Serotec) to analyze the expression of the Vβ3 TCR

EBV HLA-DR1 B cells from a homozygous patient were cultured in U-bottom wells at 2.0 $\times$ 10^5 cells/well for 120 h with or without Ags $OVA_{323–339}$ and $HA_{307–319}$ (40 μg/ml). The EBV cells were irradiated (10,000 rad) after 120 h. MDaAPC were prepared as above (26). CH7C17 T cells were incubated with MDaAPCs or natural APC for 60 h at 37°C in the presence of CO_2. CH7C17 T cells/APC were cultured at the ratio of 1:1

in the presence of IL-2 (0.8 μl per 200-μl U-bottom well). C7CH17 T cells were incubated with MDaAPC as described above (26). Expression of CD69 was assessed by FACS (FACSCalibur; BD Biosciences) using standard procedures.

Visualization of PKCθ translocation and measurement of liposomes by confocal fluorescence microscopy

FACS-sorted CD4$^+$ T cells were incubated with aAPC for 20 min and then placed on a poly-L-lysine-coated glass slide, fixed, permeabilized, and stained with polyclonal anti-PKCθ Ab (Santa Cruz Biotechnology). After washing in 1% BSA in PBS, samples were incubated with a secondary Ab coupled with Alexa 594 (Molecular Probes) and washed again. After the final wash, cells were mounted using a drop of Aqua-Poly/mount (Polysciences). Samples were viewed with a Plan-Apochromat $\times$63 lens on a Nikon microscope. Images were taken using the Bio-Rad MRC 1024 laser scanning confocal imaging system. To determine the size of liposomes, a Jurkat T cell mutant, CH7C17, was used (27). Cells were treated as described above. Single-frame confocal images were obtained by confocal videomicroscopy (LSM 410; Zeiss) using a $\times$40 lens and $\times$4 zoom for a 64-s scanning time. For measurement purposes, an Improved Neubauer hemacytometer (Reichert) was used, visualizing a square of 5-μm size.

Measurement of PKCθ capping area

The area of PKCθ translocation was measured by drawing a circle around each cell and around high-density pixel areas identified by the software using standard settings. Such high-density areas corresponded to PKCθ patches. The ratio between the outlined areas was calculated using a MetaMorph Imaging System, version 3.5 (Universal Imaging). The area of each PKCθ patch was expressed as a percentage of the whole cell area. Evaluation was performed by a blinded observer.

Statistics

Analysis of statistical significance was performed by using the Student's *t* test and calculation of linear regression and correlation coefficients between the percentage of IL-2-producing or the percentage of CD69-expressing T cells, and the immune synapse areas was calculated with Apple Works 6 (Apple) and Primers of Biostatistic software.

Results

Characterization of MDaAPC

We have previously described aAPC in which MHC-peptide complexes were randomly distributed within the bilayer membrane (16, 17, 28). In aAPC tested here (MDaAPC), MHC-peptide complexes and accessory molecules were organized into MDs within the aAPC surface.

Figure 1*a* shows a scheme of the minimum MD unit. Average size for MDaAPC was determined to be in the range between 100 and 1000 nm by confocal microscopy (Fig. 1*b*) and was confirmed by comparison to beads of known size by FACS analysis. To achieve a very high density of T cell ligands, we engineered MDaAPC to take advantage of the binding of CTB to ganglioside GM1, a component of lipids rafts in natural membranes (29, 30). GM1-containing liposomes were loaded with a preassembled tetravalent structure consisting of NA core complexes with biotinylated T cell ligands (e.g., anti-CD3 Ab or MHC-peptide complexes and anti-CD28 Abs). This structure was then anchored at the GM1/cholesterol-enriched areas of the liposome bilayer through a biotinylated CTB unit. All of the components of this aAPC were titrated to test the functionality of the system. This structure ensures appropriate orientation of the molecules involved. This represents a significant improvement over several similar technologies, including our own previously described aAPC. Each aAPC contained $\sim 8 \times 10^7$ molecules of sialo-GM1 ganglioside. At this concentration, the addition of

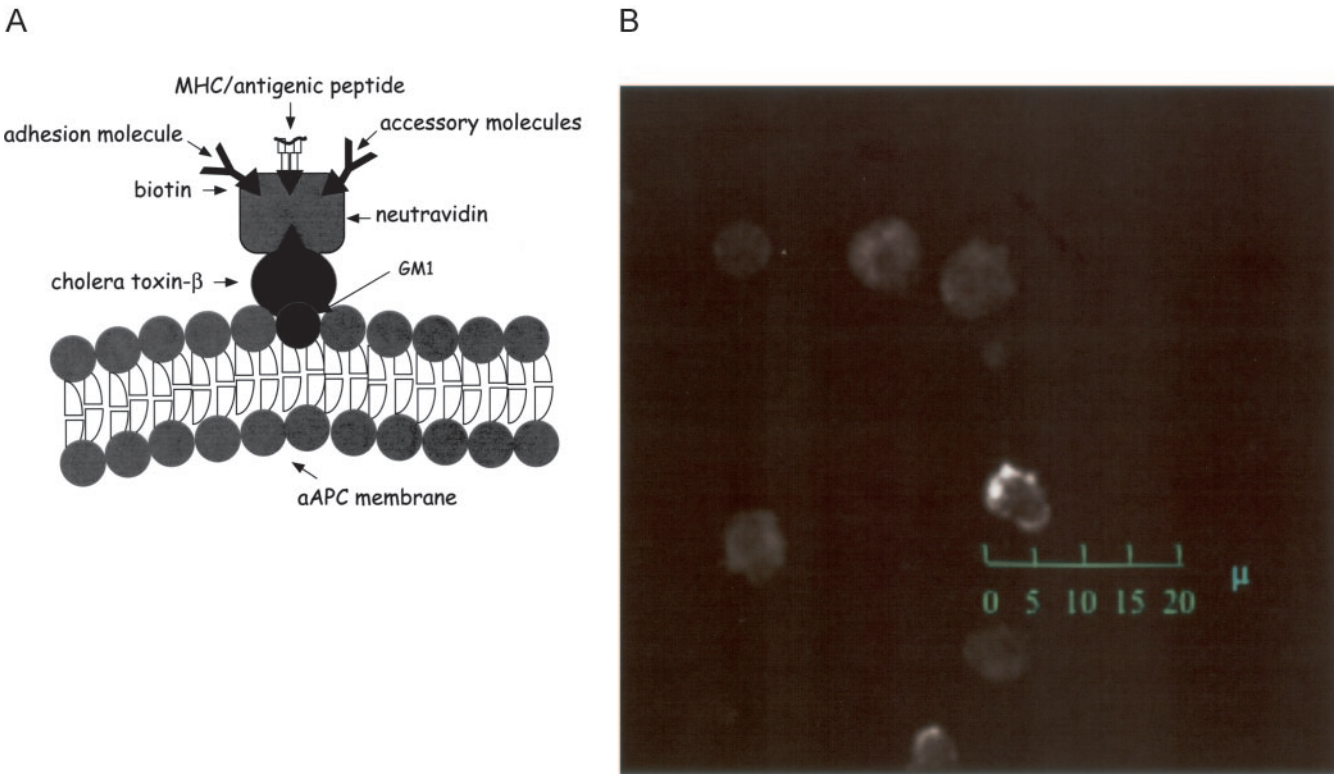

FIGURE 1. *a,* Structure of MDs on aAPC. GM1 ganglioside is part of the lipid bilayer and binds one molecule of biotinylated CTB. In each MD, one molecule of NA anchors the biotinylated molecules to the aAPC surface through one biotinylated CTB. In this specific example, the three free valences of NA are saturated with the MHC-HA peptide complex, anti-CD28 Ab, and an accessory molecule. Different combination and ratios of T cell ligands can be loaded on the MD as needed. *b,* Measurement of liposomes attached to CH7C17 cells by comparison to known size Neubauer hemacytometer using confocal videomicroscopy. CH7C17 cells were visualized by confocal videomicroscope (Zeiss) with a $\times$40 enlargement lens and enhanced by $\times$4 zoom. Single-frame images of cells were obtained at 64-s scanning time under the same conditions. Measurement was extrapolated by the known size of the hemacytometer square visualized in the same conditions (50 μm) and applied to the cells image.

Table I. *Stimulation of human CD4$^+$-sorted T cells by aAPC with anti-CD3 and anti-CD28 Abs in micromembrane domains (MDaAPC), with anti-CD3-coated beads, or with a combination of anti-CD3 Abs coated on plates and soluble anti-CD28*[a]

	CD69	IL-2
MDaAPC anti-CD3/CD28	27.9 ± 4.9 ($p < 0.03$ vs anti-CD3 beads)	13.9 ± 1.9
Anti-CD3 beads	6.69 ± 1.1	Not determined
Anti-CD3 on plates + anti-CD28 soluble	17.9 ± 1.4	12 ± 2.8
MDaAPC anti CD19 only	1.4 ± 0.3	0.6 ± 0.2
Unstimulated CD4 cells	1.3 ± 0.2	1.6 ± 0.4

[a] MDaAPC containing only the irrelevant anti-CD19 Ab and unstimulated cultures were used as controls. Values are expressed as percentage of CD4$^+$ T cells as measured by FACS analysis. Values shown are the averages from eight independent experiments using two different donors.

GM1 at 2.5–5 molar % to phosphatidylcholine/cholesterol mono- or bilayered artificial membranes leads to the formation of discrete submicrometer-sized round domains (2.5-nm thick), analogous to those found in detergent-insoluble membrane fractions. The addition of CTB increases the domain thickness to 6–7 nm, indicating an interaction of CTB subunits with GM1 hydrophilic residues on the membrane surface (31, 32).

Based on the average MDaAPC size, we estimated that the GM1 molecule density on the MDaAPC surface ranged from 60 to 600 GM1 molecules/nm^2. A 1:110 molar ratio of CTB:GM1 provided optimal T cell binding and activation rates in preliminary experiments (data not shown). The estimated CTB density on the aAPC surface ranged between 0.6 and 6 CTB/ nm^2. aAPC were labeled with FITC-conjugated CTB for visualization of aAPC binding to T cells by FACS.

Engineered aAPC are efficient in T cell stimulation in vitro

We first evaluated the efficiency of MDaAPC to induce Ag-independent activation of CD4$^+$-sorted polyclonal T cells. Stimulation of FACS-sorted CD4$^+$T cells with aAPC carrying anti-CD3 and anti-CD28 Abs on MD was compared with stimulation of the same CD4$^+$ T cells by anti CD3-coated beads or by anti-CD3-coated plates plus soluble anti-CD28 (Table I). A significantly higher percentage of CD4$^+$ T cells expressed CD69 when stimulated with aAPC carrying anti-CD3 and anti-CD28 Abs on MDs, compared with stimulation by anti-CD3 coated beads ($p < 0.03$; Table I). Figure 2 shows FACS plots for a representative experiment. Comparable values in the production of IL-2 and expression of CD69 were found upon incubation of CD4$^+$-sorted T cells with either aAPC loaded with anti-CD3 and anti-CD28 on MDs or with systems employing anti-CD3-coated plates and soluble anti-CD28 Abs (Table I). Engineered aAPC carrying the irrelevant Ab anti-CD19 alone on the MDs were used as controls and induced background T cell activation. Altogether, these data show that MDaAPC are at least as efficient as conventional methods in stimulating CD4$^+$ T cells in an Ag-independent fashion.

MDaAPC are efficient in Ag-specific ex vivo stimulation of a $HA_{307–319}$-specific human T cell line

We next compared the ability of MDaAPC and natural APC to stimulate a human T cell line in an Ag-specific fashion. To this end, we used the CH7C17 T cell line, which is specific for $HA_{307–319}$ peptide in the context of HLA DR1. We stimulated C7CH17 for 60 h with MDaAPC or natural APC loaded with the relevant Ag or with the irrelevant control peptide $OVA_{323–339}$.

Activation was measured as the percentage of CD4$^+$ T cells induced to express the activation marker CD69. As shown in Table II, a sizable activation was achieved when compared with background or the irrelevant control. No significant differences in CD69 expression were found when MDaAPC stimulation was compared with stimulation of C7CH17 with homologous natural APC loaded with either the relevant peptide or the irrelevant controls (Table II).

These results suggest that engineering T cell ligands in micromembrane domains to mimic the supramolecular organization found in natural APC could lead to comparable efficiency in ex vivo Ag-specific stimulation.

Preclustering of T cell ligands on the membrane of the aAPC affects efficiency of T cell stimulation

Ag-specific activation of CD4$^+$ human polyclonal T cells by different types of aAPC was studied in response to influenza peptide $HA_{307–319}$. FACS-sorted CD4$^+$ T cells from HLA-DRB1*0701 and HLA-DRB1*1101 donors previously immunized with influenza vaccine were stimulated by using MHC-$HA_{307–319}$ class II

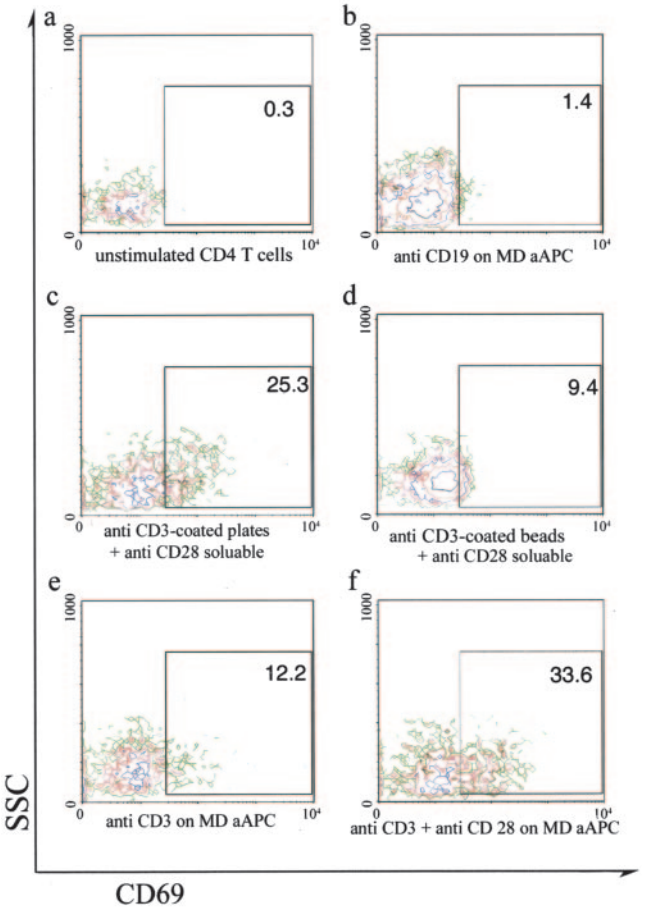

FIGURE 2. Representative FACS experiments showing percentages of sorted CD4$^+$ human cells stimulated in various conditions, as specified. aAPC contained MDs.

Table II. *Stimulation of human $HA_{307–319}$-specific human T cell line by natural APC or MDaAPC*[a]

	MDaAPC	Natural APC
Medium	13.96 ± 3.63	12.60 ± 0.16
$OVA_{323–339}$	14.48 ± 0.97	15.47 ± 2.96
$HA_{307–319}$	53.20 ± 4.35	57.27 ± 0.62

[a] Readout as percentage of $CD4^+$ T cells expressing the activation marker CD69 after 60 h of incubation with natural APC or MDaAPC loaded with the relevant Ag ($HA_{307–319}$) or with the irrelevant control peptide $OVA_{323–339}$. Numbers represent the mean ± SD of two independent experiments.

complexes loaded on aAPC or organized in soluble tetramers. Intensity of responses was compared between aAPC with MHC-peptide complexes clustered on MDs or randomly distributed within the aAPC membrane. To compare aAPC with autologous APC-induced activation, total PBMC from both donors were stimulated in vitro for 60 h with $HA_{307–319}$ peptide at 10 μg/ml. Negative controls included sorted $CD4^+$ T cells stimulated with MDaAPC containing either anti-CD19 or anti-CD28. MHC class II molecules used were either affinity-purified C-terminal-biotinylated DRB1*0701 obtained from a human B cell line expressing DRB1*0701 or recombinant biotinylated HLA-DRB1*1101. Percentages of CD69 and IL-2-positive cells were measured by FACS analysis on gated $CD4^+$ T cells (Fig. 3 as summary of eight independent experiments and Fig. 4 showing FACS plots of one representative experiment). Expression of CD69 was significantly higher when aAPC containing MHC/$HA_{307–319}$ plus anti-CD28 organized into MDs were used, as compared with aAPC containing MHC/$HA_{307–319}$ in addition to anti-CD28 randomly distributed on the aAPC surface (Fig. 3*a*, $p < 0.05$). Similarly, IL-2 production was also significantly higher using aAPC containing MHC/$HA_{307–319}$ in addition to anti-CD28 organized into MDs vs aAPC containing MHC/$HA_{307–319}$ in addition to anti-CD28 randomly distributed on the

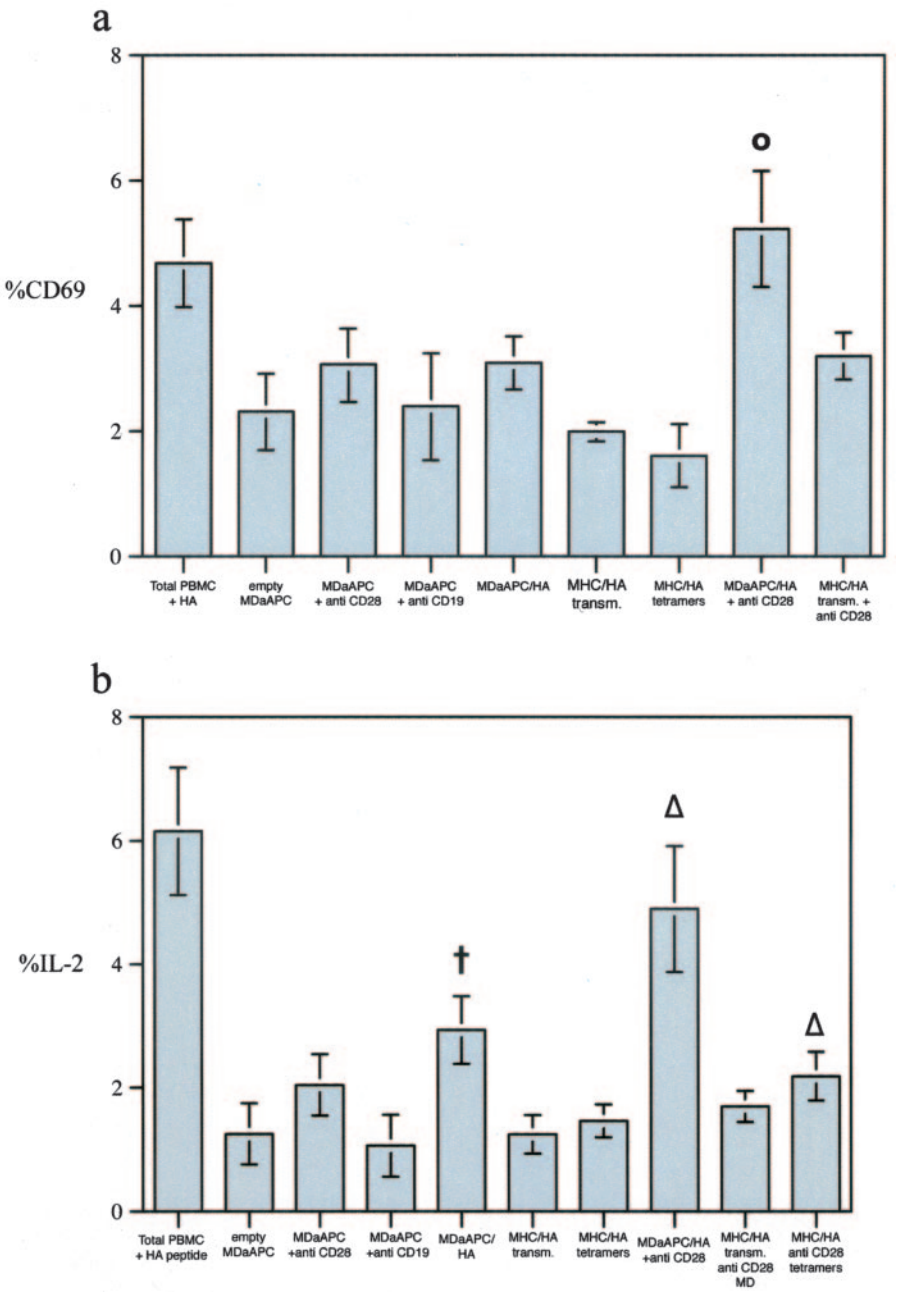

FIGURE 3. Percentages of $CD4^+$ T cells and expressing CD69 producing IL-2 upon stimulation with aAPC. *a,* The percentage of $CD4^+$ T cells producing CD69 upon stimulation was significantly higher with aAPC carrying MHC/HA + anti-CD28 organized into MDs compared with aAPC carrying MHC/HA + aCD28 randomly distributed in the membrane (*, $p < 0.05$). *b,* The percentage of $CD4^+$ T cells producing intracellular IL-2 upon stimulation with aAPC carrying MHC/HA organized into MDs was significantly higher when compared with MHC/HA randomly distributed on the aAPC membrane (*, $p < 0.012$). Additionally, a significant increase was also seen with aAPC with MHC/HA + anti-CD28 organized into MDs compared with aAPC carrying MHC/HA + aanti-CD28 randomly distributed in the membrane (*, $p < 0.009$). Total PBMC incubated for 60 h with 10 μg/ml $HA_{307–319}$ peptide were used as positive control of stimulation. Control aAPC included aAPC carrying anti-CD28 or anti-CD19 on MDs. Bars indicate the averaged values calculated from $n = 8$ experiments ± SD.

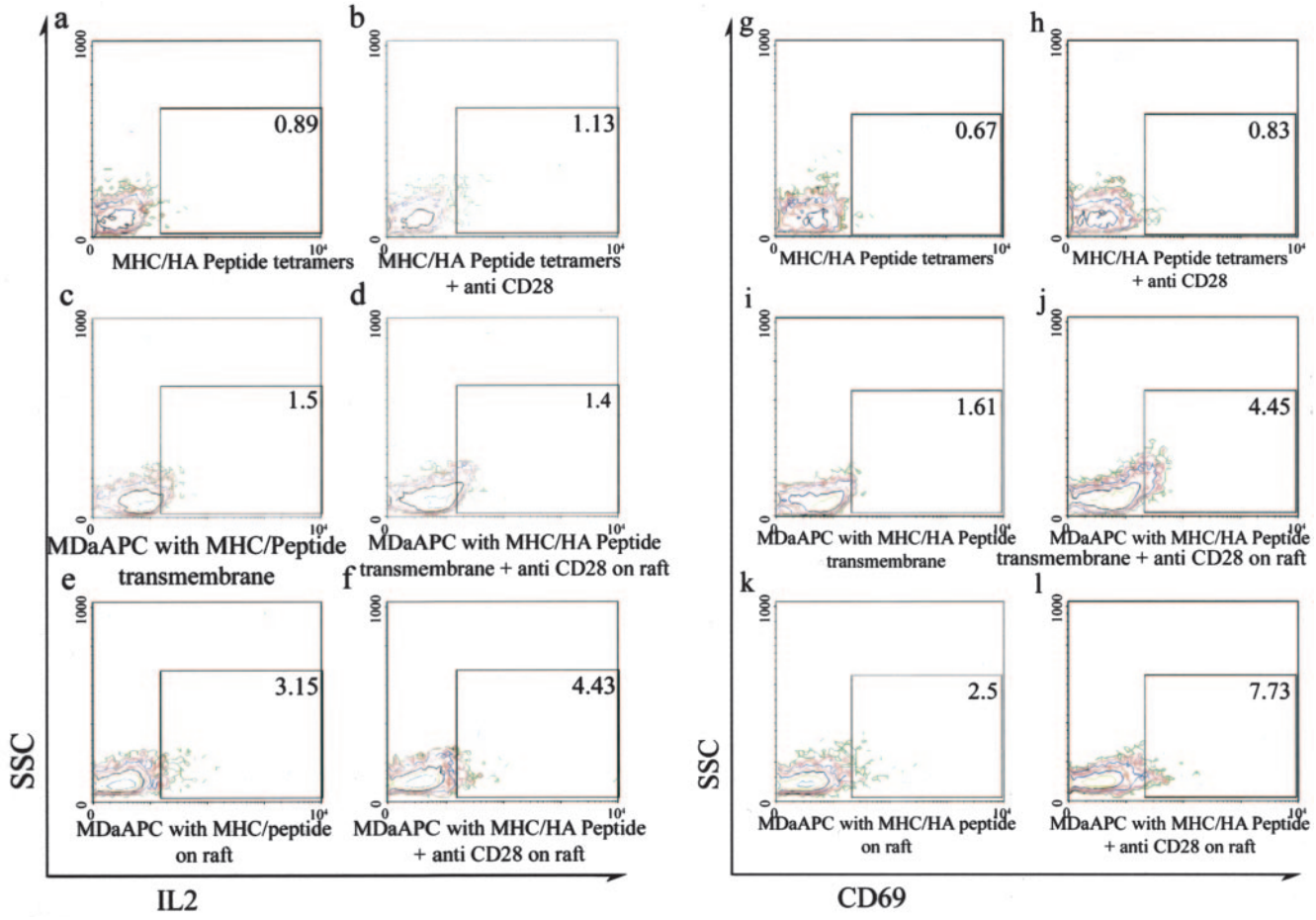

FIGURE 4. FACS analysis of intracellular IL-2 production by presorted $CD4^+$T cells upon different activating conditions. Intracellular production of IL-2 and expression of CD69 by presorted $CD4^+$ T cells stimulated for 60 h in the presence of aAPC or MHC/peptide (HA) tetramers. FACS plots from one representative experiment show the percentage of IL-2-producing $CD4^+$T cells (*a–f*) and CD69 (*g–l*).

aAPC surface (Fig. 3*b*, $p < 0.009$). The efficiency of both aAPC types in stimulating Ag-specific T cells was higher than the one obtained with soluble MHC/HA tetramers (Figs. 3 and 4), with or without anti-CD28 (3 mol of MHC/HA moles and 1 mol of anti-CD28 mole per mole of NA). No differences were observed between affinity-purified biotinylated DRB1*0701 and recombinant biotinylated HLA-DRB1*1101 in the efficiency of stimulating $HA_{307–319}$-specific $CD4^+$ T cells (data not shown).

Organization of T cell ligands on aAPC membranes affects PKCθ translocation

We then analyzed whether the supramolecular organization of T cell ligands on the surface of aAPC was associated with effective triggering of the physiological signaling pathways that lead to full T cell activation. To address this issue, we chose to correlate the level of translocation of PKCθ to the T cell plasma membrane upon interaction with the two different types of aAPC. PKCθ plays an essential role in T cell activation. Upon TCR engagement by its ligand, PKCθ translocates from the cytosol to membrane lipid rafts clustering at the IS and colocalizing with TCR in the central core of the SMAC (1). PKCθ translocation is also directly associated with IL-2 production and T cell activation. Hence, PKCθ recruitment to the membrane could be correlated with physiological IS assembly and TCR signaling (33, 34). Translocation of PKCθ was analyzed by confocal microscopy in FACS-sorted $CD4^+$ T cells from influenza-immunized individuals after a 20-min incubation with various types of aAPC (Fig. 5). After cell fixation and permeabilization, endogenous PKCθ was stained with a specific Ab. PKCθ was homogeneously distributed in the cytosol in $CD4^+$ T cells incubated with MDaAPC carrying an irrelevant Ab (anti-CD19) (Fig. 5*a*). Conversely, PKCθ was translocated to discrete plasma membrane patches in $CD4^+$ T cells incubated with MDaAPCs loaded with DRB1*0701/HA complexes alone (Fig. 5*b*) or with DRB1*0701/HA in combination with anti-CD28 on the MDaAPC (Fig. 5*c*). Incubation of $CD4^+$ T cells with aAPC carrying HLADRB1*0701-HA complexes randomly distributed in the lipid bilayer (Fig. 5*d*) induced a lesser degree of PKCθ translocation in membrane patches, underscoring the functional significance of membrane MDs. As previously shown (16), capping on the T cell membrane colocalized with the area of interaction between T cell and aAPC. Fig. 5*e* shows a T cell with PKCθ stained red with Alexa Red and a cluster of aAPC stained with FITC-conjugated CTB (green).

To analyze the differences in the magnitude of the PKCθ translocation in the $CD4^+$T cells incubated with aAPC or MDaAPC, we measured the area of PKCθ patches formed at the T cell membrane level in a semiquantitative fashion. The relative area of PKCθ translocation was measured by calculating the ratio of the total cell area to the area of PKCθ patching and expressed as the percentage of the whole cell area. High-density pixel areas were identified by the software using standard settings. The ratios were calculated by MetaMorph Imaging System, version 3.5 (Universal Imaging). The area of each PKCθ patch was expressed as percentage of the whole cell area. A comparable number of cells was

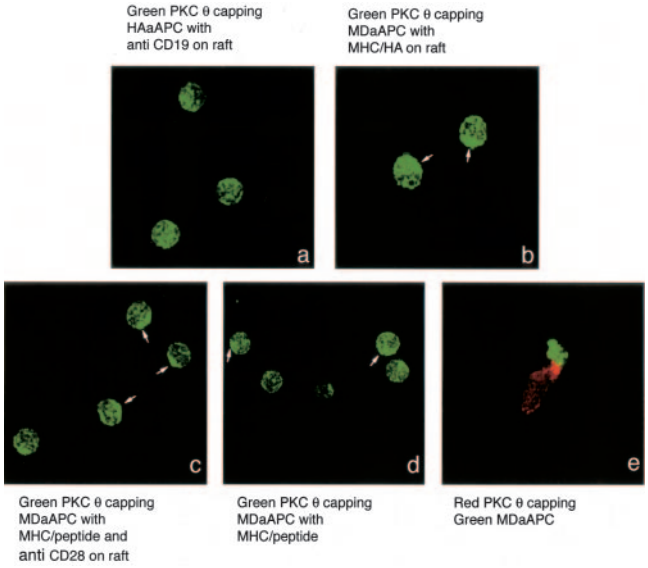

FIGURE 5. Confocal microscopy images of PKCθ translocation to membrane patches. PKCθ capping is visualized by staining with a FITC-conjugated secondary Ab (*a–d*, in green). Arrowheads indicate PKCθ capping, defined as described. *e,* Interaction of aAPC (stained with FITC-conjugated CTB, green) and a T cell (PKCθ capping stained with an Alexa-conjugated secondary Ab, red).

analyzed in each condition. Evaluation was performed by an observer blinded to the identity of the samples. MDaAPC containing anti-CD19 and anti-CD28 were used as controls to define the background surface distribution of PKCθ. PKCθ patched areas were significantly wider when cells were stimulated with MHC-HA complexes loaded on MDs rather than when they were randomly distributed on the aAPC membrane ($p < 0.001$, Table III).

These data indicate that preclustering of MHC-peptide complexes into high-density MDs on the aAPC surface may contribute to the extent of PKC translocation and therefore to effective engagement of signaling pathways leading to T cell activation. In fact, it has been shown that expression of IL-2 and CD69 is regulated by the binding of NF-κB and AP-1 transcription factors to specific consensus binding sites on IL-2 and CD69 gene promoters (35, 36). Since PKCθ integrates downstream the TCR and CD28-derived activation signals by inducing activation and nuclear translocation of NF-κB and AP-1 (37, 38), the expression of genes involved in T cell activation might be correlated with the level of PKCθ translocation at the IS. In fact, we found a statistically significant positive correlation between the PKCθ capping area and the percentage of IL-2-producing $CD4^+$ T cells ($r = 0.85$, $p < 0.01$). The percentage of $CD4^+$ T cells expressing CD69 showed also a significantly positive correlation with PKCθ capping area ($r = 0.83$, $p < 0.04$).

Discussion

Induction and modulation of Ag-specific T cell responses is a complex multistep process. T cells specific for a given Ag must "sample" several APC to allow encounter with the appropriate Ag (39–41). This process is based on multiple, short-lived, "exploratory" contacts that get stabilized by clustering of relevant molecules upon the interaction of the TCR with its specific MHC-peptide combination on the APC surface. It has been shown that T cells can engage APC and disengage from it even after a few minutes of interaction to bind APC with a higher representation/relative density of the relevant MHC-peptide combination (39–41). A growing body of evidence supports the concept that clustering of T cell ligands is important to effectively engage and activate Ag-specific T cells. The dishomogeneous distribution of T cell ligands on the membrane of APC may precisely serve the purpose to provide high-density areas to enhance the chance of a stable interaction, leading to T cell activation. This concept is still not fully proven, given the difficulty in manipulating composition and relative concentration of membrane-bound molecules in natural APC. This work was undertaken to address directly the issue of effects on T cell responsiveness of relative organization (not absolute concentration) of T cell ligands on the APC membrane. We were able to demonstrate directly, using two artificial systems which we have developed, that mimicking the organization in MDs found in natural APC gives a distinct advantage in T cell stimulation. T cell responses were mirrored by PKCθ capping at the level of T-aAPC interaction areas. It is of interest to note that these correlations were obtained in entirely artificial systems by manipulating the level of organization of T cell ligands on the membrane, not their concentration, since amounts of reagents were identical between MD-aAPC and aAPC.

Table III. *Semiquantitative measurement of PKCθ capping*[a]

	Relative Area
Empty MDaAPC ($n = 31$)	14.7 ± 1.3
MDaAPC anti-CD19 and anti-CD28 ($n = 34$)	15.3 ± 1.2
aAPC MHC/HA ($n = 23$)	17 ± 0.8
MDaAPC MHC/HA ($n = 17$)	24.7 ± 0.9 ($p < 0.001$ vs aAPC same composition)
aAPC MHC/HA and anti-CD28 ($n = 49$)	20.7 ± 2.2
MDaAPC MHC/HA and anti-CD28 ($n = 39$)	25.1 ± 2 ($p < 0.001$ vs aAPC same composition)

[a] Relative areas were determined as described and represent the averages of the ratio between the total area and the area of PKCθ capping (high pixel density areas) studied per condition (n).

The fact that we can control in an entirely artificial system molarity and relative concentrations of T cell ligands provides, in our opinion, a useful tool for basic science as well as medical applications. In our own experience (Ref. 26 and S. Albani, unpublished data), MDaAPC are an excellent tool to expand and modulate ex vivo Ag-specific T cells which are rare or otherwise difficult to grow. The use of MD-aAPC is particularly attractive for modulation ex vivo of T cell responses in therapy of cancer and infectious diseases. For instance, several clinical trials which use *Drosophila*-transfected or autologous Ag-loaded dendritic cells for ex vivo stimulation of T cells have shown promising preliminary results, particularly in melanoma and B cell lymphoma. Substantial problems have, however, plagued these attempts, in particular given the difficulties in standardization and the potential for xenoreactions in the case of nonhuman cells.

In summary, these data provide support for the concept that Ag-specific activation of polyclonal T cells may be positively affected by preclustering of T cell ligands. We propose here an entirely artificial system that enables the organization of relevant T cell ligands into membrane MDs and allows for manipulation of molarity, relative density, and affinity to achieve physiological Ag presentation.

Acknowledgments

We thank Dr. Silvia Albani for art work and Peter Zieseniss for image editing.

Disclosures

S. Albani disclosed delivering expert testimony or involvement in patents received or pending.

References

1. Xavier, R., T. Brennan, Q. Li, C. McCormack, and B. Seed. 1998. Membrane compartmentation is required for efficient T cell activation. *Immunity 8:723*.
2. Janes, P. W., S. C. Ley, and A. I. Magee. 1999. Aggregation of lipid rafts accompanies signaling via the T cell antigen receptor. *J. Cell Biol. 18:447*.
3. Langlet, C., A. M. Bernard, P. Drevot, and H. T. He. 2000. Membrane rafts and signaling by the multichain immune recognition receptors. *Curr. Opin. Immunol. 12:250*.
4. Monks, C. R., B. A. Freiberg, H. Kupfer, N. Sciaky, and A. Kupfer. 1998. Three-dimensional segregation of supramolecular activation clusters in T cells. *Nature 395:82*.
5. Grakoui, A., S. K. Bromley, C. Sumen, M. M. Davis, A. S. Shaw, P. M. Allen, and M. L. Dustin. 1999. The immunological synapse: a molecular machine controlling T cell activation. *Science 285:221*.
6. Bromley, S. K., W. R. Burack, K. G. Johnson, K. Somersalo, T. N. Sims, C. Sumen, M. M. Davis, A. S. Shaw, P. M. Allen, and M. L. Dustin. 2001. The immunological synapse. *Annu. Rev. Immunol. 19:375.*
7. Dustin, M. L. 2002. Regulation of T cell migration through formation of immunological synapses: the stop signal hypothesis. *J. Clin. Invest. 109:155*.
8. Krummel, M. F., and M. M. Davis. 2001. Dynamics of the immunological synapse: finding, establishing and solidifying a connection. *Curr. Opin. Immunol. 14:66*.
9. Jenei, A., S. Varga, L. Bene, L. Matyus, A. Bodner, Z. Basco, C. Pieri, R. Gaspar, Jr., T. Farkas, and S. Damjanovich. 1997. HLA class I and II antigens are partially co-clustered in the plasma membrane of human lymphoblastoid cells. *Proc. Natl. Acad. Sci. USA 94:7269*.
10. Faroudi, M., R. Zaru, B. Favier, and S. Valitutti. 2002. New insights to the functional role of the T cell-antigen presenting cell immunological synapse. *Biol. Res. 35:133*.
11. Wulfing, C., C. Sumen, M. D. Sjaastad, L. C. Wu, M. L. Dustin, and M. M. Davis. 2002. Costimulation and endogenous MHC ligands contribute to T cell recognition. *Nat. Immunol. 3:42*.
12. Hackett, C. J., and O. K. Sharma. 2002. Frontiers in peptide-MHC class II multimer technology. *Nat. Immunol. 3:887*.
13. Watts, T. H. 1988. T cell activation by preformed, long-lived Ia-peptide complexes: quantitative aspects. *J. Immunol. 141:3708*.
14. Harding, C. V., and E. R. Unanue. 1990. Quantitation of antigen-presenting cell MHC class II/peptide complexes necessary for T-cell stimulation. *Nature 346:574*.
15. Oelke, M., M. V. Maus, D. Didiano, C. H. June, A. Mackensen, and J. P. Schneck. 2003. Ex vivo induction and expansion of antigen specific cytotoxic T cells by HLA-Ig-coated artificial antigen-presenting cells. *Nat. Med. 9:619*.
16. Prakken, B., M. Wauben, D. Genini, R. Samodal, J. Barnett, A. Mendivil, L. Leoni, and S. Albani. 2000. Artificial antigen-presenting cells as a tool to exploit the immune "synapse." *Nat. Med. 6:1406*.
17. Massa, M., N. Costouros, F. Mazzoli, F. De Benedetti, A. La Cava, T. Le, I. De Kleer, A. Ravelli, M. Liotta, S. Roord, et al. 2002. Self epitopes shared between human skeletal myosin and *Streptococcus pyogenes* M5 protein are targets of immune responses in active juvenile dermatomyositis. *Arthritis Rheum. 46:3015*.
18. Mallet-Designe, V. I., T. Stratmann, D. Homann, F. Carbone, M. B. Oldstone, and L. Teyton. 2002. Detection of low-avidity $CD4^+$ T cells using recombinant artificial APC: following the antiovalbumin immune response. *J. Immunol. 170:123*.
19. Vogt, A. B., S. Spindeldreher, and H. Kropshofer. 2002. Clustering of MHC-peptide complexes prior to their engagement in the immunological synapse: lipid raft and tetraspan microdomains. *Immunol. Rev. 189:136*.
20. Anderson, H. A., E. M. Hiltbold, and P. A. Roche. 2000. Concentration of MHC class II molecules in lipid rafts facilitates antigen presentation. *Nat. Immunol. 2:156*.
21. Setterblad, N., S. Becart, D. Charron, and N. Mooney. 2001. Signalling via MHC class II molecules modifies the composition of GEMs in APC. *Scand. J. Immunol. 54:87*.
22. Kropshofer, H., S. Spindeldreher, T. A. Rohn, M. Platania, C. Grygar, N. Daniel, A. Wolpl, H. Langen, V. Horejsi, and A. B. Vogt. 2002. Tetraspan microdomains distinct from lipid rafts enrich select peptide-MHC class II complexes. *Nat. Immunol. 3:61*.
23. Machy, P., K. Serre, M. Baillet, and L. Leserman. 2002. Induction of MHC class I presentation of exogenous antigen by dendritic cells is controlled by $CD4^+$ T cells engaging class II molecules in cholesterol-rich domains. *J. Immunol. 168:1172*.
24. Kwok, W. W., A. W. Liu, E. J. Novak, J. A. Gebe, R. A. Ettinger, G. T. Neopam, S. N. Raymond, and D. M. Koelle. 2000. HLA-DQ tetramers identify epitope-specific T cells in peripheral blood of herpes simplex virus type 2-infected individuals: direct detection of immunodominant antigen-responsive cells. *J. Immunol. 164:4244*.
25. Kwok, W., N. Ptacek, A. Liu, and J. Buckner. 2002. Use of class II tetramers for identification of $CD4^+$ T cells. *J. Immunol. Methods 268:71*.
26. Prakken, B. J., R. Samodal, T. D. Le, F. Giannoni, G. P. Yung, J. Scavulli, D. Amox, S. Roord, I. de Kleer, D. Bonnin, et al. 2004. Epitope-specific immunotherapy induces immune deviation of proinflammatory T cells in rheumatoid arthritis. *Proc. Natl. Acad. Sci. USA 101:4228.*
27. Cameron, T. O., P. J. Norris, A. Patel, C. Moulon, E. S. Rosenberg, E. D. Mellins, L. R. Wedderburn, and L. J. Stern. 2002. Labeling antigen-specific $CD4^+$ T cells with class II MHC oligomers. *J. Immunol. Methods 268:51*.
28. Bonnin, D., B. J. Prakken, R. Samodal, A. La Cava, D. A. Carson, and S. Albani. 1999. Ontogeny of synonymous T cell populations with specificity for a self MHC epitope mimicked by a bacterial homologue: an antigen-specific T cell analysis in a non-transgenic system. *Eur. J. Immunol. 29:3826*.
29. Goebel, J., K. Forrest, D. Flynn, R. Rao, and T. Roszman. 2002. Lipid rafts, major histocompatibility complex molecules, and immune regulation. *Hum. Immunol. 63:813*.
30. Simons, K., and E. Ikonen. 1997. Functional rafts in cell membranes. *Nature 387:569*.
31. Hering, H., C. C. Lin, and M. J. Sheng. 2003. Lipid rafts in the maintenance of synapses, dendritic spines, and surface AMPA receptor stability. *J. Neurosci. 23:3262.*
32. Yuan, C., and L. J. Johnston. 2001. Atomic force microscopy studies of ganglioside GM1 domains in phosphatidylcholine and phosphatidylcholine/cholesterol bilayers. *Biophys. J. 81:1059*.
33. Altman, A., N. Isakov, and G. Baier. 2000. Protein kinase Cθ: a new essential superstar on the T-cell stage. *Immunol. Today 21:567*.
34. Bi, K., Y. Tanaka, N. Coudronniere, K. Sugie, S. Hong, M. J. van Stipdonk, and A. Altman. 2001. Antigen-induced translocation of PKC-θ to membrane rafts is required for T cell activation. *Nat. Immunol. 2:556*.
35. Viola, A., S. Schroeder, Y. Sakakibara, and A. Lanzavecchia. 1999. T lymphocyte costimulation mediated by reorganization of membrane microdomains. *Science 283:680*.
36. Coudronniere, N., M. Villalba, N. Englund, and A. Altman. 2000. NF-κB activation induced by T cell receptor/CD28 costimulation is mediated by protein kinase C-θ. *Proc. Natl. Acad. Sci. USA 97:3394*.
37. Sun, Z., C. W. Arendt, W. Ellmeier, E. M. Schaeffer, M. J. Sunshine, L. Gandhi, J. Annes, D. Petrzilka, A. Kupfer, P. L. Schwartzberg, and D. R. Littman. 2000. PKC-θ is required for TCR-induced NF-κB activation in mature but not immature T lymphocytes. *Nature 404:402*.
38. Dennehy, K. M., A. Kerstan, A. Bischof, J. H. Park, S. Y. Na, and T. Hunig. 2003. Mitogenic signals through CD28 activate the protein kinase Cθ-NF-κB pathway in primary peripheral T cells. *Int. Immunol. 15:655*.
39. McBride, J. M., and C. G. Fatham. 2002. A complicated relationship: fulfilling the interactive needs of the T lymphocyte and the dendritic cell. *Pharmacogenomics J. 2:367*.
40. Dustin, M. L., P. M. Allen, and A. S. Shaw. 2001. Environmental control of immunological synapse formation and duration. *Trends Immunol. 22:192*.
41. Underhill, D. M., M. Bassetti, A. Rudensky, and A. Aderem. Dynamic interactions of macrophages with T cells during antigen presentation. *J. Exp. Med. 12:1909.*